



HAL
open science

Electrochemistry Visualization Tool to Support the Electrochemical Analysis of Batteries

Matheus Leal de Souza, Marc Duquesnoy, Mathieu Morcrette, Alejandro Franco

► **To cite this version:**

Matheus Leal de Souza, Marc Duquesnoy, Mathieu Morcrette, Alejandro Franco. Electrochemistry Visualization Tool to Support the Electrochemical Analysis of Batteries. Batteries & Supercaps, 2022, 10.1002/batt.202200378 . hal-03878812

HAL Id: hal-03878812

<https://hal.science/hal-03878812v1>

Submitted on 2 Dec 2022

HAL is a multi-disciplinary open access archive for the deposit and dissemination of scientific research documents, whether they are published or not. The documents may come from teaching and research institutions in France or abroad, or from public or private research centers.

L'archive ouverte pluridisciplinaire **HAL**, est destinée au dépôt et à la diffusion de documents scientifiques de niveau recherche, publiés ou non, émanant des établissements d'enseignement et de recherche français ou étrangers, des laboratoires publics ou privés.



Distributed under a Creative Commons Attribution 4.0 International License

Electrochemistry Visualization Tool to Support the Electrochemical Analysis of Batteries

Matheus Leal de Souza,^[a,b] Marc Duquesnoy,^[a,c] Mathieu Morcrette,^{*[a,b,c]} and Alejandro A. Franco^{*[a,b,c,d]}

- [a] M. Leal de Souza, M. Duquesnoy, Dr. M. Morcrette, Prof. Dr. A. A. Franco
Laboratoire de Réactivité et Chimie des Solides (LRCS),
UMR CNRS 7314, Université de Picardie Jules Verne,
Hub de l'Énergie, 15 rue Baudelocque, 80039 Amiens Cedex, France
E-mails: mathieu.morcrette@u-picardie.fr, alejandro.franco@u-picardie.fr
- [b] M. Leal de Souza, Dr. M. Morcrette, Prof. Dr. A. A. Franco
Réseau sur le Stockage Electrochimique de l'Énergie (RS2E),
FR CNRS 3459, Hub de l'Énergie, 15 rue Baudelocque, 80039 Amiens Cedex, France
- [c] M. Duquesnoy, Dr. M. Morcrette, Prof. Dr. A. A. Franco
ALISTORE-European Research Institute, FR CNRS 3104
Hub de l'Énergie,
15, rue Baudelocque, 80039 Amiens Cedex, France
- [d] Prof. Dr. A. A. Franco
Institut Universitaire de France
103 Boulevard Saint Michel, 75005 Paris, France

Abstract: To meet the expected performance requirements of lithium-ion batteries (LIBs), novel electrode materials, coatings and electrolytes have been studied in terms of their degradation mechanisms. Nevertheless, most of the methods used to track these mechanisms are not *in operando*, i.e. they do not follow them upon the practical LIB cell operation. The differential voltage analysis (DVA) and the incremental capacity analysis (ICA) constitute *in operando* techniques that can greatly help in monitoring batteries degradation mechanisms. We report here an *in house* developed software that allows the visualization of the DVA and the ICA curves of tested cells, with the possibility of rebuilding an experimental full-cell capacity vs. potential curve through fitting of its electrodes' half-cell capacity vs. potential curves. Those features can be applied to multiple charge-discharge cycles without data pretreatment, offering data exportation. We illustrate the functionalities of our software and indicate perspectives for its further development.

Introduction

Lithium ion batteries (LIBs) are among the most used family of batteries for electronic portable devices, electric vehicles and grid energy storage systems. Despite of their relative high energy density and adaptability to a wide spectrum of applications, their present stage of development still falls short of what is needed for the upcoming demands from renewable energy sources. Higher energy densities, higher power performances (for fast charge purposes), an expanded cycle life upon charge and discharge and a safer operation specially for larger scales are still challenges to overcome to improve LIBs competitiveness.^[1-3]

Novel electrolytes, electrode coatings, Ni-richer positive electrodes and use of silicon as partial replacement for graphite in negative electrodes are some of the approaches being undertaken by the research community to address these challenges. However, every new approach to improve LIB performance faces its own set of degradation mechanisms, typically very complex due to the involvement of numerous mechanisms and parameters which influence the overall LIB behavior. Dendrite formation, Li plating, dissolution of transition metals, Solid Electrolyte Interphase (SEI) formation and growth, loss of contact between electrode and current collector and particles cracking are some of the reasons for cells capacity and power fading.^[4-6] The detection and tracking of those events is therefore essential to accurately boost the improvement of performance and produce reliable LIB cells. In this context, the analysis of the dynamics of the potential vs. capacity curves along aging or cycling for that goal is far from being fully exploited, though its features can bring information about capacity loss from each electrode, chemistry change and lithium inventory, all related to degradation mechanisms.^[4,7]

At fixed temperature and sufficiently low current density, the active materials show a characteristic potential vs. capacity curve whose features can be unraveled by using two techniques: Incremental Capacity Analysis (ICA) or dQ/dV vs. V , and Differential Voltage Analysis (DVA) or dV/dQ vs. Q .^[8-10]

ICA emphasizes the mostly horizontal regions of the potential vs. capacity curve of a cell and as its x-axis is the potential, this technique shows to be a powerful tool for half-cells once the position, the height and the set of the peaks are directly related to information about impedance evolution, mass loss and chemistry change of one electrode.^[11,12] Nevertheless, ICA information for full-cell is non-trivial to be obtained, demanding convolutions of the electrodes properties. Despite of that, there exist models that are based on the ICA in full-cells to track degradation mechanisms such as loss of lithium inventory, ohmic resistance increase and loss of active material.^[13-16]

DVA emphasizes the mostly vertical regions of the potential vs. capacity curve of a cell and its x-axis, differently of ICA, is the capacity, which decreases upon degradation. One advantage of this technique though is conserving the approximate linear relations of electrode potential to the full-cell potential of Eq. (1) for their derivatives, as in Eq. (2), considering negligible impedance contributions:

$$V_{cell} = V_{pos} - V_{neg} \quad \text{Eq. (1)}$$

$$\frac{dV_{cell}}{dQ} = \frac{dV_{pos}}{dQ} - \frac{dV_{neg}}{dQ} \quad \text{Eq. (2)}$$

Those relations allow the reconstruction of a full-cell potential vs. capacity curve from the half-cells curves of its electrodes using their total capacities (proportional to the electrode mass) and their relative capacity displacement, also known as slippage, as parameters of the fitting.^[17–25]

For each of those techniques there are already available support tools, as the case of alawa toolbox of the University of Hawai'i at Manoa, which uses ICA coupled with a diagnostic and prognostic model^[14,15] and of VAWQuum Dalhousie University freeware, which uses DVA for the fitting of the full-cell curve with the half-cell references and also presents the visualization of the ICA of the cells.^[21] To further help that electrochemical analysis, herein we describe the Electrochemistry Visualization Application (EVA), a program developed for the visualization of the potential vs. capacity, ICA and DVA curves; the reconstruction of a full-cell curve through fitting of the half-cells curves; and the data export. The possibility of simultaneous visualization of the potential vs. capacity and both the differential techniques by selection in a friendly interface for the fitting turns the analysis more intuitive. Additionally, those functions are possible for multiple cycles and without the need of data pretreatment for BioLogic EC-Lab[®] Software entry data, turning EVA a powerful and practical tool for the user.

Description of the Program

The design of the application is based on PyQt5, a well-known comprehensive set of Qt5 application packages and Python bindings, offering modules for the development of multi-platform desktop Graphical User Interface (GUI) applications, including Windows, Unix and Mac OS.^[26,27] The main modules of PyQt5 embed functionalities like the QtCore, a module for the assessment of data types, files, or directories. QtGui has dedicated functionalities to structure the window-based application with common graphics, fonts and 2D plots. QtWidgets offers tools to create the different styles and objects for the GUI. The front-end and the back-end of the GUI are both developed using Python 3.7, embedding the detailed modules above to deal with the treatment of the electrochemical data. In our case study, we developed the application ready to be used under Windows 10 and Unix platforms.^[27]

In this GUI, the user loads the electrochemical results coming from EC-Lab[®] software (treated as .mpt files) in order to analyze automatically without manual settings, the capacity and voltage values included into such type of files that are not easy to handle from a common desktop program. In this regard, the GUI facilitates the pre-treatment and post-treatment of the electrochemical curves using dedicated Python classes from the back-end, storing and retrieving the measurements from the files, but also the fitting processes that are proposed by the GUI. When the user is satisfied with the extraction of data and the calculations of fittings, the GUI offers different 2D representations to render plots implemented using PyQt5 toolkits which embed *matplotlib* modules.

Program Functionalities

Once EVA is initialized, the first step to be taken is to load the entries. The present alpha version of EVA accepts up to three files simultaneously as entries. They are labeled “Positive”, “Negative” and “Full”, meaning a positive electrode half-cell, a negative electrode half-cell and the full-cell, respectively. All of them can be generated through saving as .mpt file any EC-Lab[®] galvanostatic cycling with potential limitation (GCPL) raw data containing solely constant current charge and discharge cycling profiles. These files contain from the recorded points of the cycling information such as current, potential, time and capacity. For positive electrode half-cell and full-cell data, the cycle is taken as a charge phase followed by a discharge phase while for negative electrode half-cell data it's the opposite since in half-cell the negative electrode of the full-cell is the positive electrode (once commonly Li is used as a counter electrode whose potential is the lowest available). Each of these entries is independently uploaded to the program through selecting the option “File”, followed by the option “Ageing” and then the option “Protocols”, in which a browser will open to access the files location once their proper label (Positive, Negative or Full) is assigned (see Figure 1).

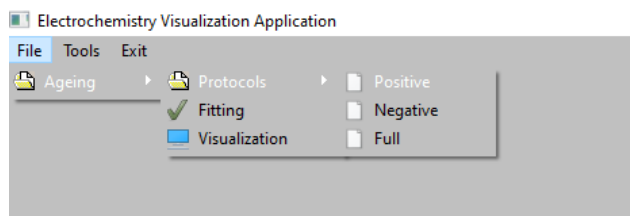


Figure 1. EVA ageing functions bar selected for entries loading.

To illustrate the functionalities of EVA, three coin cells of 14 mm of diameter electrodes were cycled at 25°C in a heating chamber and their charge-discharge data after formation cycles composed the entry files read by the software. First is the full cell, composed of a working electrode of NMC811 (7.4 ± 0.2 mg) and a counter electrode of Graphite GHDR 15-4 (4.3 ± 0.2 mg). They are separated by a fiberglass separator (Whatman) and filled with 1M LiPF₆ in EC:EMC (3:7 wt%) + 2 wt% VC. This cell was cycled between 2.50V-4.20V

at $19.99 \pm 0.01 \mu\text{A}/\text{cm}^2$. Second cell is a positive half-cell, composed of a working electrode of NMC811 ($7.8 \pm 0.2 \text{ mg}$) and a counter electrode of lithium. They are separated by a Celgard 2500 separator and filled with 1M LiPF_6 in EC:EMC (3:7 wt%) + 2 wt% VC. This cell was cycled between 2.50V-4.60V at $20.00 \pm 0.01 \mu\text{A}/\text{cm}^2$. Third cell is a negative half-cell, composed of a working electrode of Graphite GHDR 15-4 ($4.3 \pm 0.2 \text{ mg}$) and a counter electrode of lithium. They are separated by a Celgard 2500 separator and filled with 1M LiPF_6 in EC:EMC (3:7 wt%). This cell was cycled between 0.01V-1.50V at $19.72 \pm 0.01 \mu\text{A}/\text{cm}^2$.

Once the files are uploaded, the access of visualization is done through selecting the option "File", followed by the option "Ageing" and then the option "Visualization". The data graphs will be displayed by electrode selection through the option "Electrode", by cycle number if the data contains multiple cycles through "Cycle n" bar, and by the electrochemical curve through "Graph type". The graph type "V/Q" refers to the potential vs. capacity curves, being the capacity, in mAh, the unit chosen for the horizontal axis. Units as mAh/g or the state of charge (SOC) were not taken in order not to insert errors due to mass calculation and possible misunderstandings since SOC definition depends on adopted criteria (see Figures 2, 3 and 4). The graph type "ICA" refers to the dQ/dV vs. potential curves (see Figures 5, 6 and 7) and the graph type "DVA" refers to the dV/dQ vs. capacity curves (see Figures 8, 9 and 10). Referring to the latest, as well as the "V/Q" curves, the horizontal axis is the capacity, in mAh, and the vertical axis is in V/mAh. For this visualization graph type, any discharge phase is represented as $-dV/dQ$ for the vertical axis in order to coincide with the DVA plots of the fitting function as additive members of Eq. (2) Besides, no normalized representations such as SOC in the horizontal axis or $Q_0 \times dV/dQ$ (in which Q_0 is the phase total capacity) in the vertical axis are done once their eventual use in fittings difficults the general comprehension of the analysis of slippage and mass ratio variations.

For the fitting function, the three files with different labels must be previously uploaded, and an initial screen is presented upon selection of the option "File", followed by the option "Ageing" and then the option "Fitting" (see Figure 11). Therein two windows will be shown. One contains four "V/Q" curves, for the positive and negative electrodes half-cell references, the full cell and the fitting one, obtained through Eq. (1). In the case, the present version of EVA fits only the charge phase of the full cell, that is correspondent to an oxidation at the positive electrode and a reduction at the negative electrode. The second window is by default the DVA curves fitting of the four curves of the first window through Eq. (2) and for which the "Scaling" can be adjusted and the negative electrode half-cell reference ordinated is represented as its $-dV/dQ$. By choosing the ICA fitting type, as it does not present linear relations with the half-cells references, only the ICA of the full cell and from the fitting curve of the "V/Q" window are shown.

To fit, there are four parameters, two referring to each of the electrodes half-cell references curves. First parameter is the slippage, that is the relative capacity horizontal displacement of the curve of one electrode to the full cell curve reference. The default value for the slippage is 0 mAh and by changing it the curves slide horizontally to negative values of the capacity axis. The mass ratio parameter refers to the ratio between the mass of each electrode active material of the full cell compared to the mass of the half-cells references active materials.

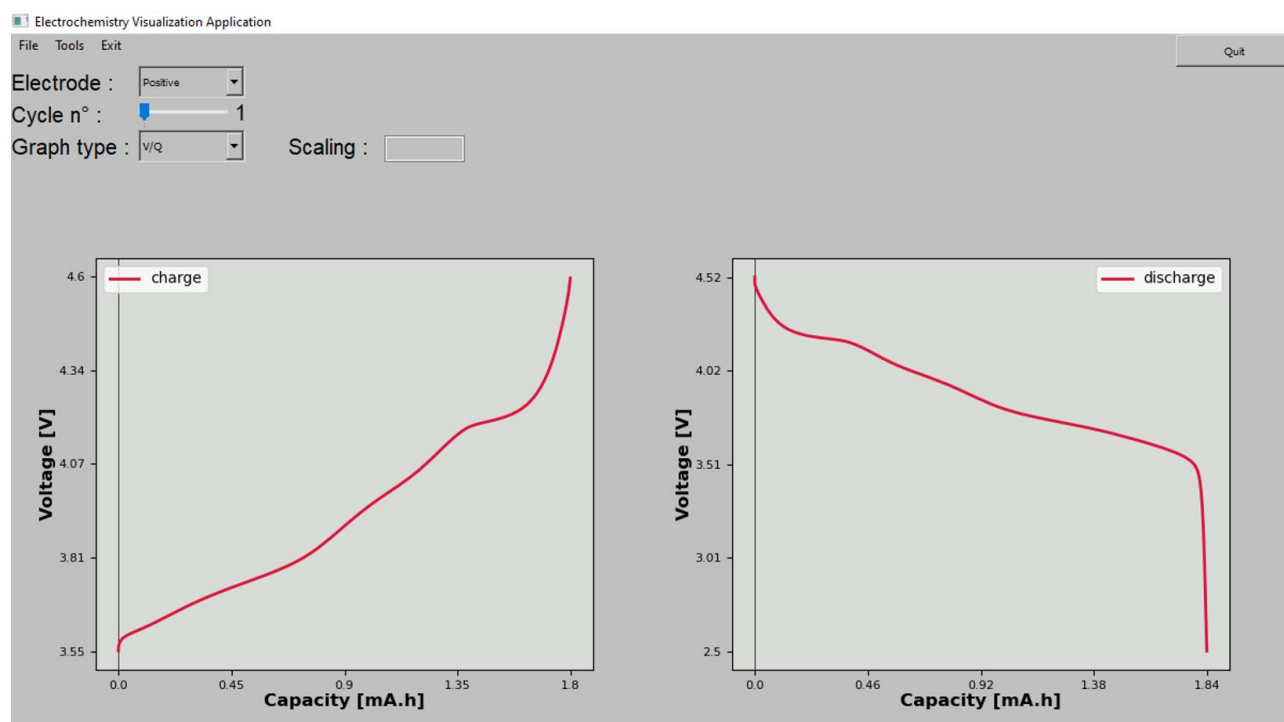


Figure 2. Potential vs. capacity visualization window for the positive electrode half-cell reference.

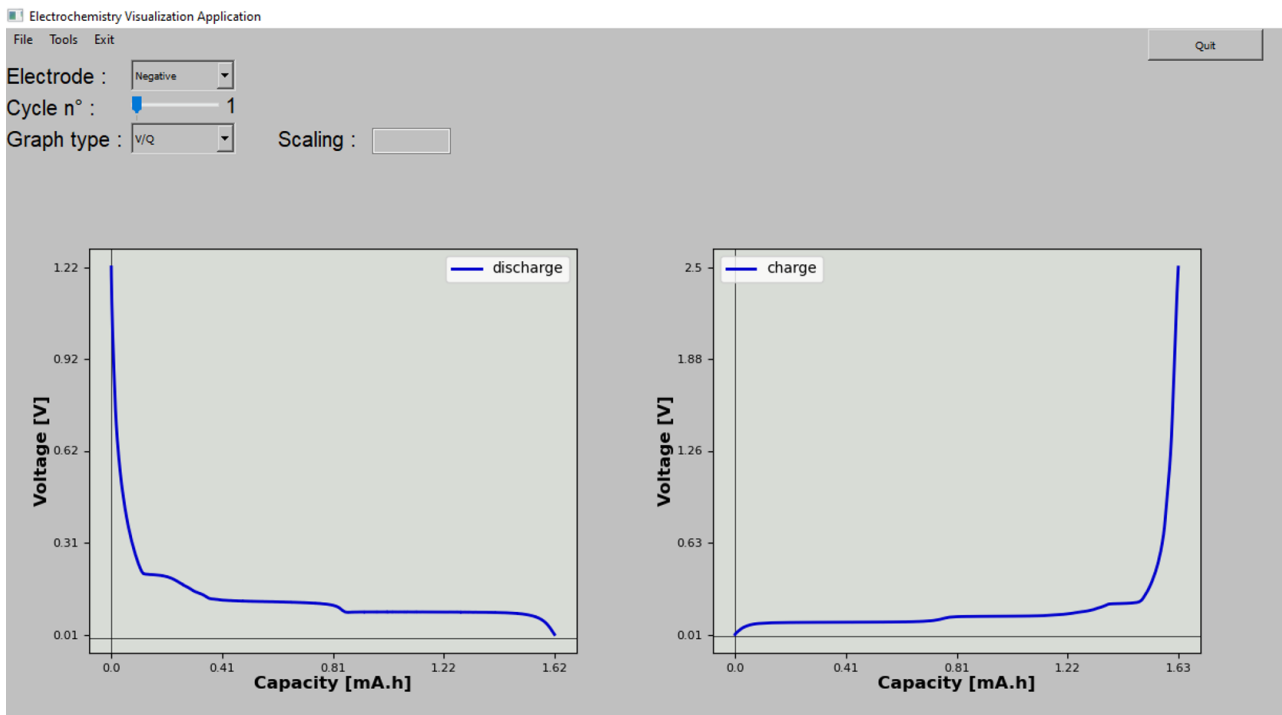


Figure 3. Potential vs. capacity visualization window for the negative electrode half-cell reference.

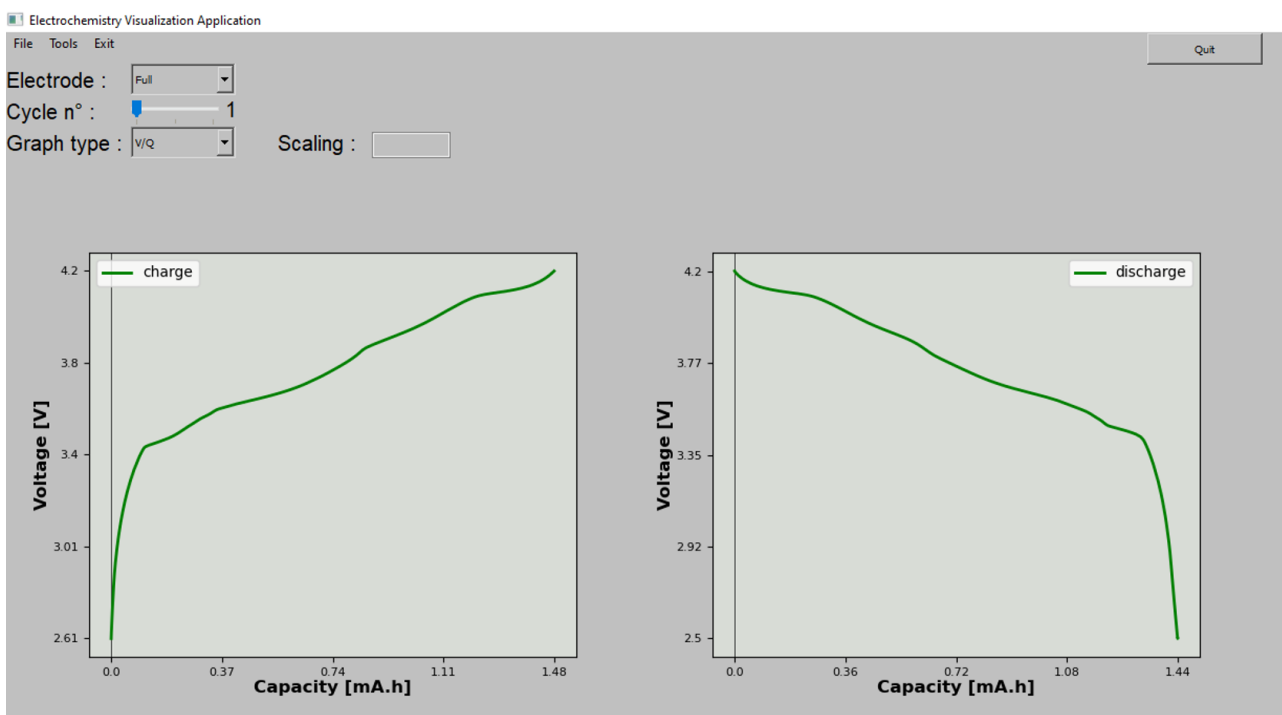


Figure 4. Potential vs. capacity visualization window for the full-cell.

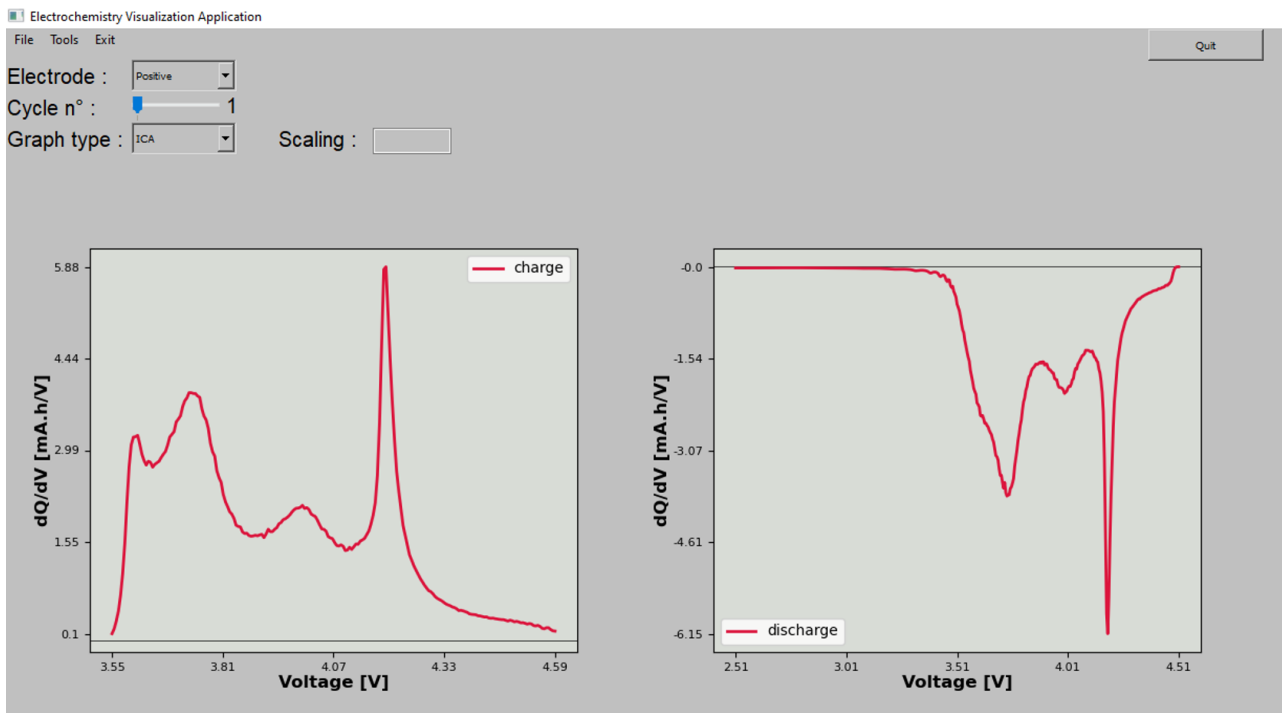


Figure 5. dQ/dV vs. potential visualization window for the positive electrode half-cell reference.

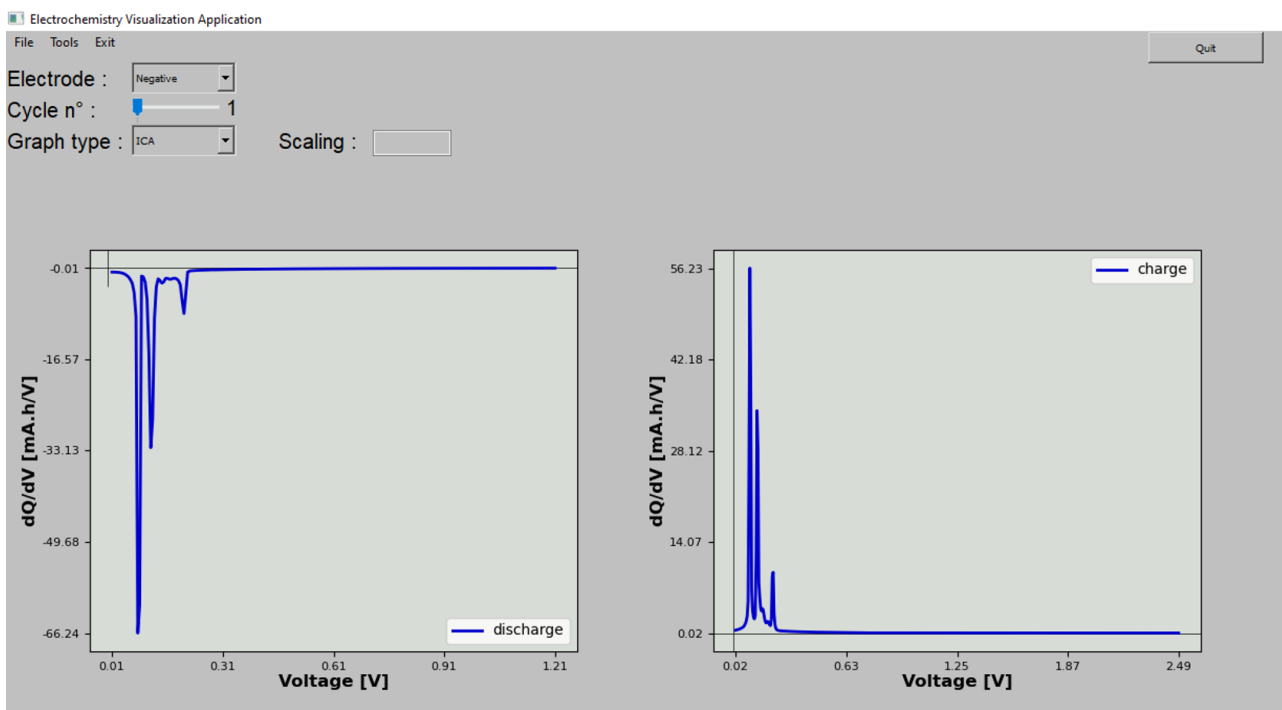


Figure 6. dQ/dV vs. potential visualization window for the negative electrode half-cell reference.

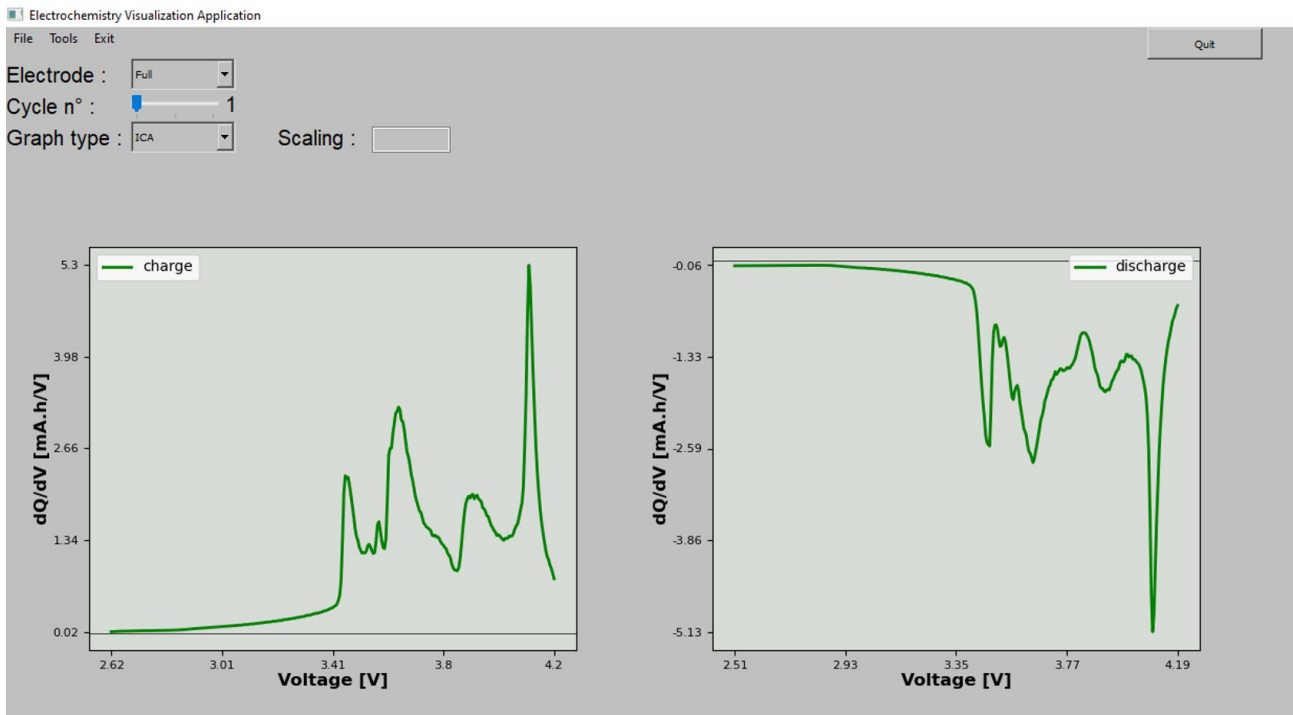


Figure 7. dQ/dV vs. potential visualization window for the full-cell.

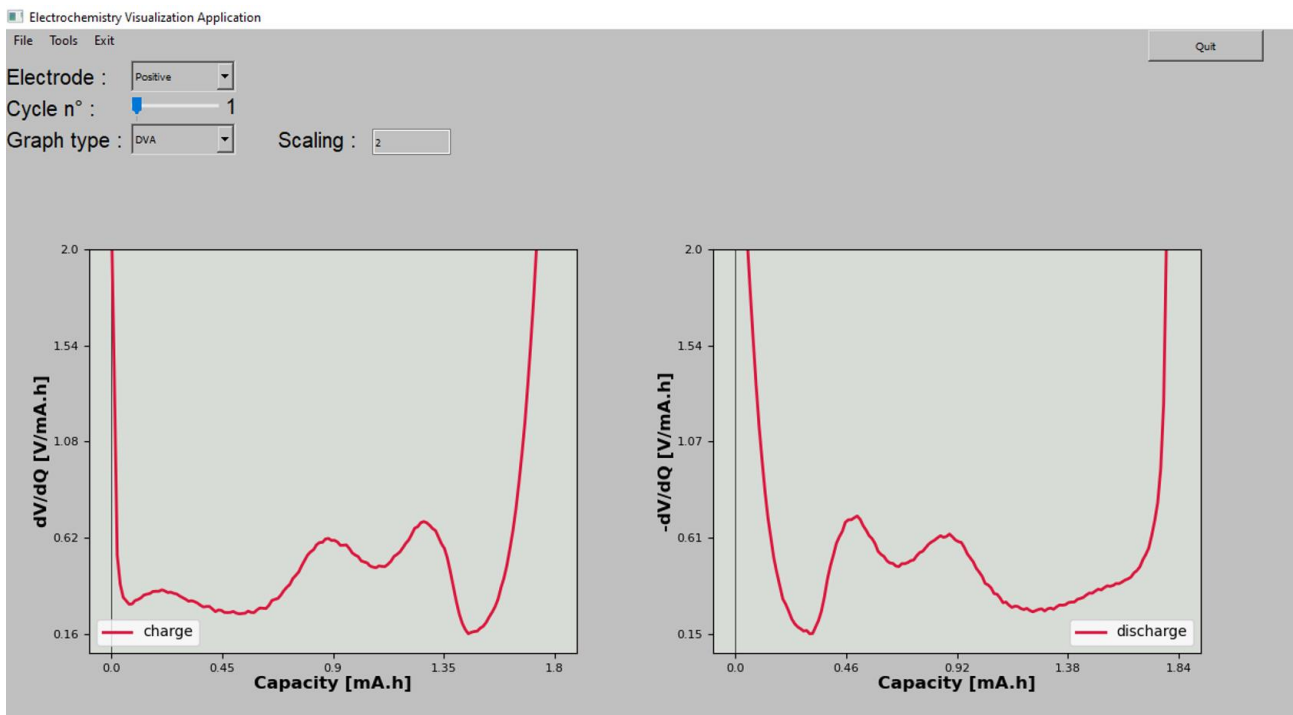


Figure 8. dV/dQ vs. capacity visualization window with the "scaling" bar adjusted to 2 V/mAh for the positive electrode half-cell reference.

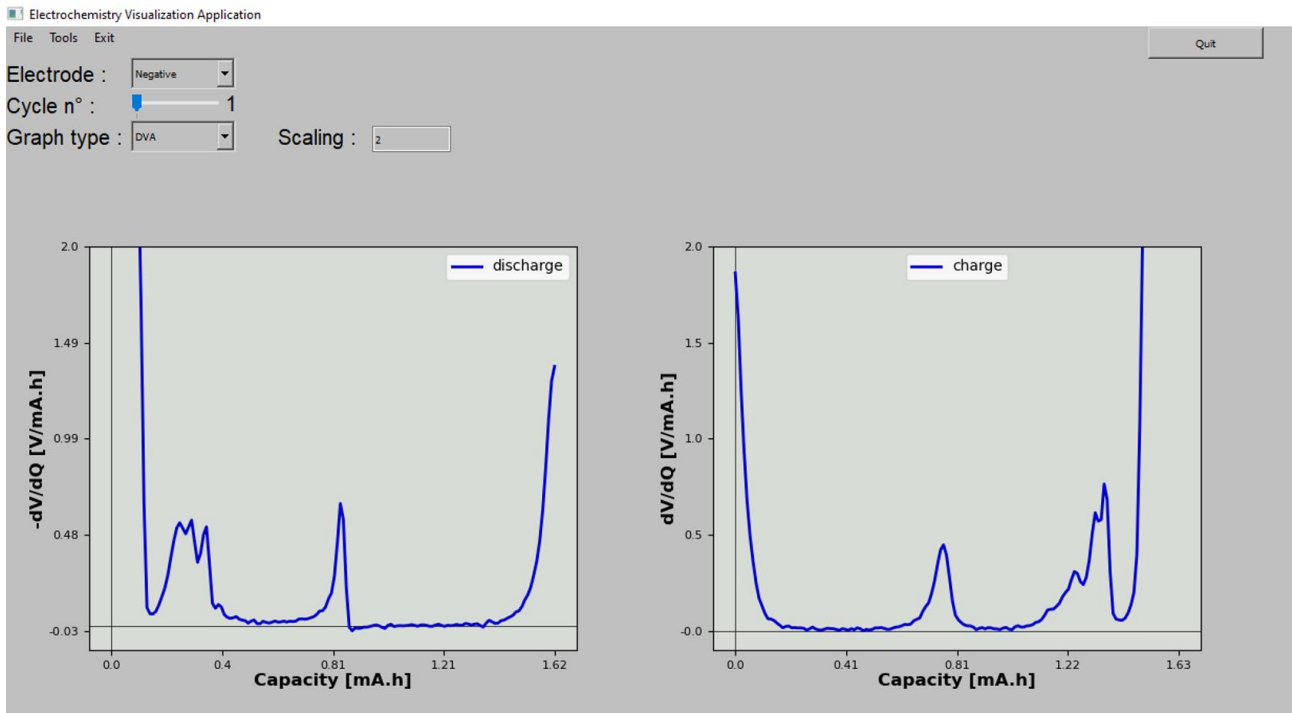


Figure 9. dV/dQ vs. capacity visualization window with the “scaling” bar adjusted to 2 V/mAh for the negative electrode half-cell reference.

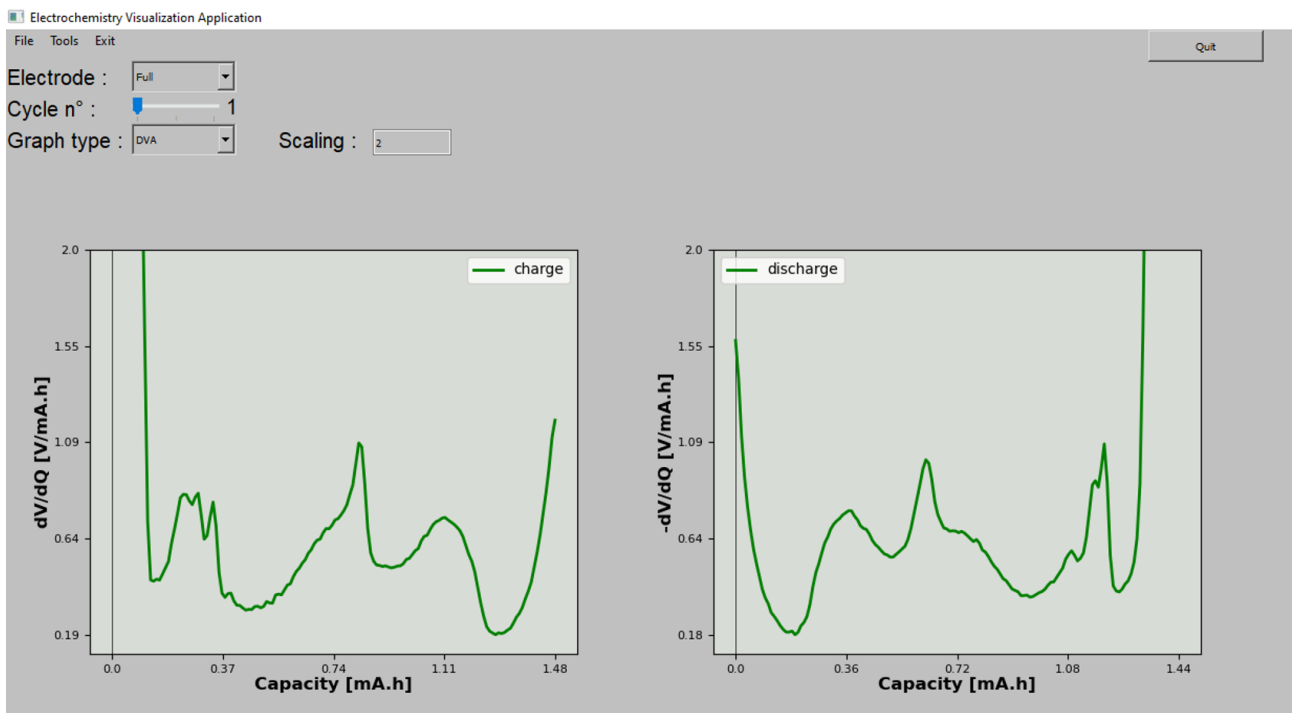


Figure 10. dV/dQ vs. capacity visualization window with the “scaling” bar adjusted to 2 V/mAh for the full-cell.

The default value for this parameter is 1 and changing it will affect the width of the capacity of the half-cell curves by shrinking or expanding them as a multiplication. The dV/dQ vertical axis of the DVA fitting type will then be inversely impacted. In fact, although being related to the mass, this parameter is a ratio between capacities. Therefore, a relative representation rather than a direct mass representation was adopted not to insert errors of mass calculation and capacities variations of sampling (e.g., in case a full cell undergoing degradation loses mass at the positive electrode, two positive electrodes reference half-cells with same capacity but slightly different masses would indicate same relative mass loss in the full cell after fitting but different absolute mass losses)

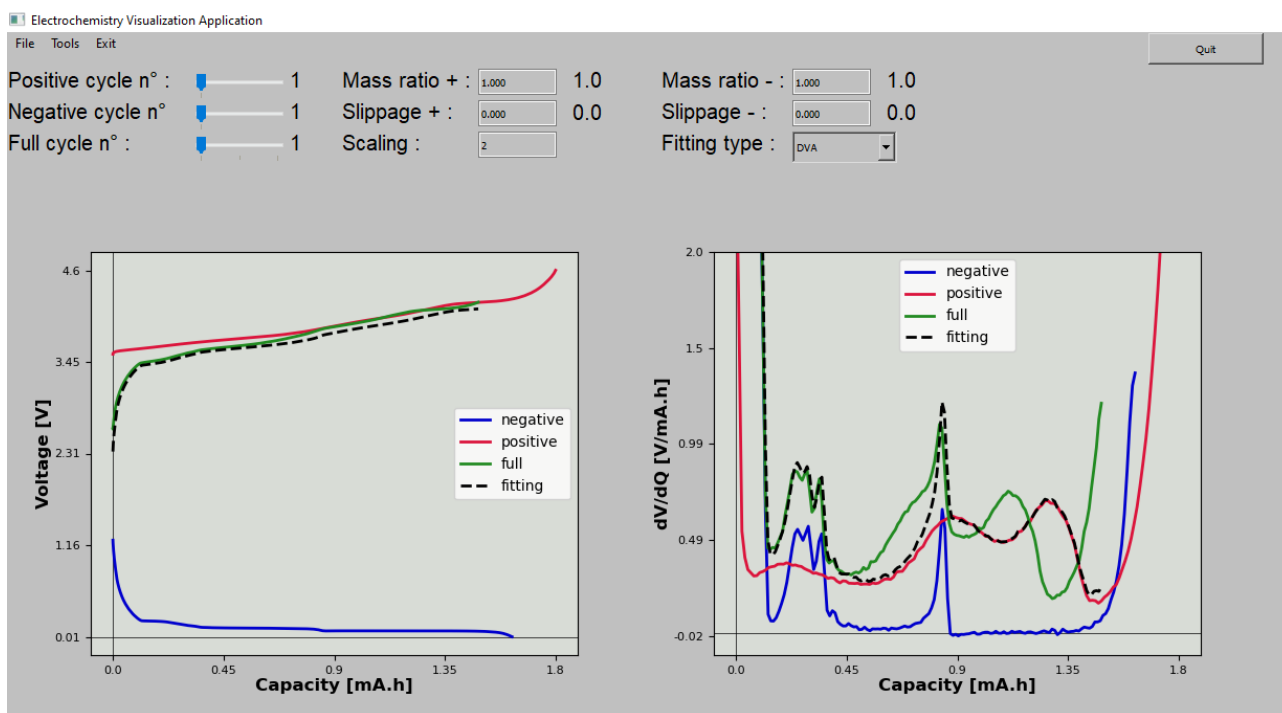


Figure 11. Fitting window for the DVA fitting type with default parameters of slippage and mass ratios. Default fitting parameters do not fit the full cell curve

In order to obtain an optimal fitting (see Figures 12 and 13), not only the aforementioned conditions for differential techniques need to be satisfied (low current densities and stable temperature) but also the similarity of conditions between the full cell electrodes and the half-cell references (current density, temperature, porosity and mass loading). Other factors such as the choice of separators, of the electrolytes and how data is recorded might impact the fitting. Even though the conditions to apply these techniques might seem restrictive, they can track degradation under multiple ageing regimes if inserted as control cycles. However, impedance rise, self-discharge and important capacity losses during the control cycle tend to make difficult the fitting once they move away from the validity of Eq. (1) and Eq. (2) or would importantly locally change the fitting parameters within a charge phase.

In Figures 12 and 13, the curves presented are obtained after 3 formation cycles and thus do not contain the initial irreversible capacity associated to each electrode during first charge. Those initial irreversible capacities though impact the initial slippage of the curves because their causes (SEI formation, limited relithiation of positive electrode, reaction of impurities and others) are directly related to cyclable lithium ion inventory. In case, the initial slippage of the negative electrode is minimal, meaning that it is practically delithiated in the beginning of the charge, while the slippage of the positive electrode is the predominant one, meaning that no further lithiation rate of the positive electrode could be reached at the end of the previous discharge. An increase of the positive slippage along degradation would then mean that Li ions are being irreversibly consumed. Also, the initial mass ratios from the fitting of each electrode are consistent with the expected range from the scale calculated masses of half-cell references and full cell electrodes (0.943 from fitting for the positive electrode and 0.994 from fitting for the negative electrode). Along degradation, the evolution of those mass ratios will deliver mass variations for each electrode which originate from multiple reasons such as particles isolation or side reactions. Additionally, it is important to emphasize that mass variations by themselves also impact the slippage of the electrodes.

For further treatment, the user can download as .csv files the curves present in the actual screen, either for visualization or fitting. That function is accessed by selecting the option "Tools" and then the option "Download". Through selecting the option "Tools" followed by selection of the option "Help", the user will have access to a video guide for the application use.

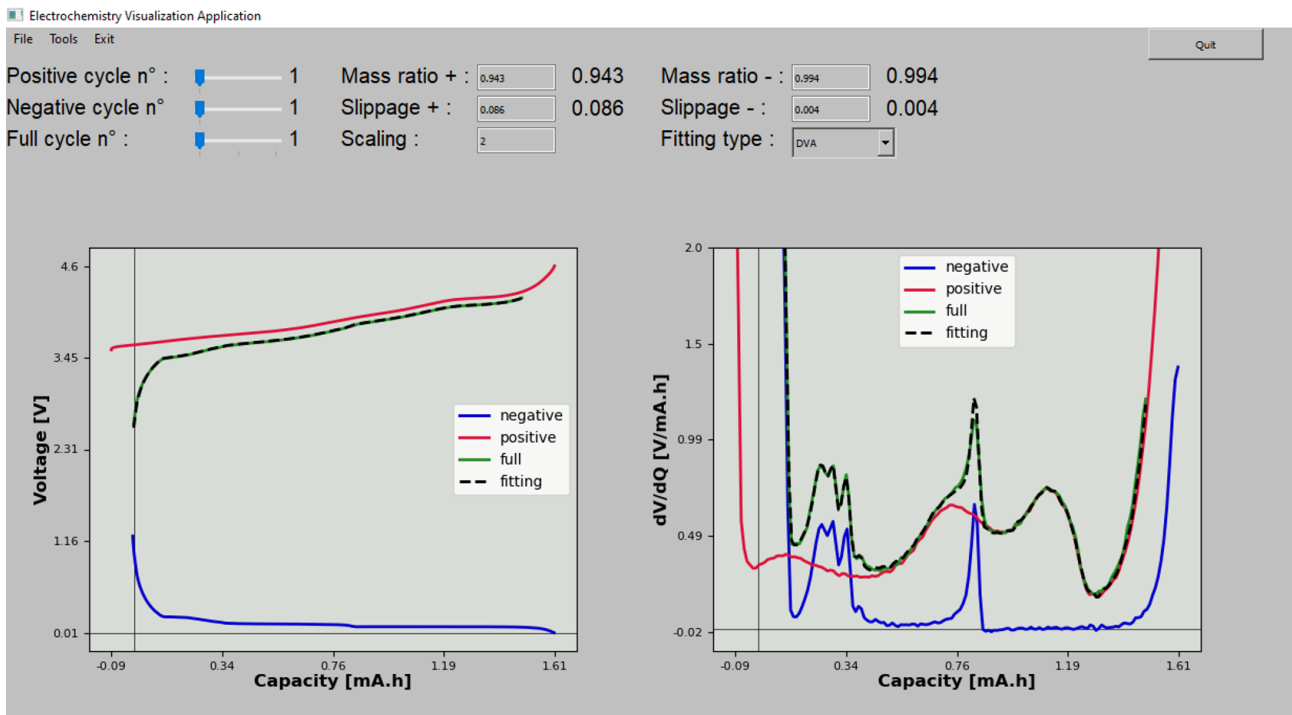


Figure 12. Fitting window for the DVA fitting type. Fitting parameters set manually in order to fit the curves.

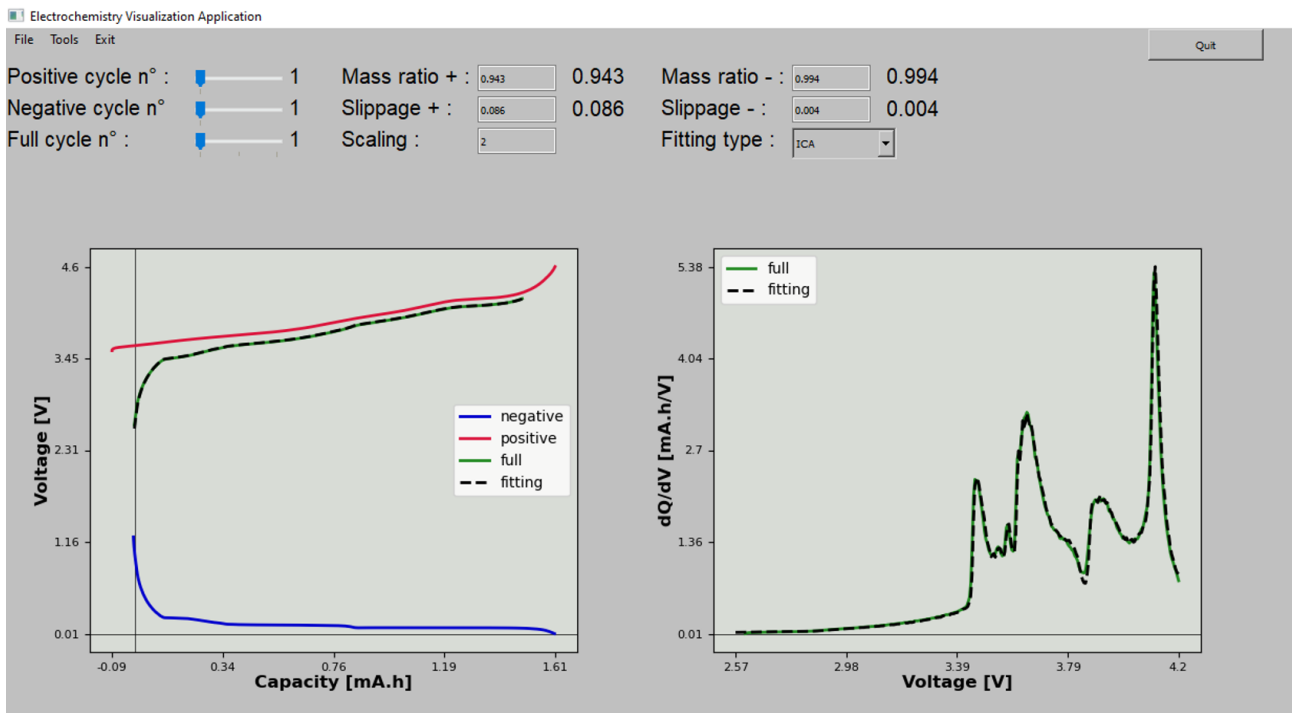


Figure 13. Fitting window for the ICA fitting type. Fitting parameters set manually in order to fit the curves.

Accessibility to the Program and Perspectives

The scientific community has a major role in developing the knowledge that serves as a basis for the technological improvement required to overcome challenges in the domain of energy storage. This domain calls for more complex and multidisciplinary expertise, which in turn demands research cooperation and information exchange but the lack of available data, communication and standards for concepts and methodologies drags the acceleration of scientific discoveries^[28]. Open science initiatives are called to fill those gaps by promoting inclusion, transparency and data reliability. As a tool to boost scientific cooperation in the field of batteries, the BIG-MAP

project^[29–32] develops an open science methodology. An illustrative example of this is the BattINFO software to support interoperability within the consortium through common ontologies^[33], following initiatives like the one preconized in materials science by the European Materials Modeling Council.^[34] EVA is available for download from a Github repository upon publication of this paper through the following URL: <https://big-map.github.io/big-map-registry/apps/EVA.html>. The application has a friendly display and a simple operation in order to support electrochemical analysis and to spread the use of the differential techniques of ICA and DVA, as well as the fitting to track degradation mechanisms. The present version of EVA to the publication also turns those analyses practical without the need of data treatment and the fitting intuitive with the addition of the capacity vs. potential fitting to the ICA or DVA fitting windows. Moreover, forthcoming upgraded versions are intended to add functionalities, rendering EVA more flexible to data entry.

Acknowledgements

The authors acknowledge the European Union's Horizon 2020 research and innovation programme for funding via the BIG-MAP project (grant agreement 957189). AAF acknowledges the support of the European Union's Horizon 2020 research and innovation program for the funding support through the European Research Council (grant agreement 772873, "ARTISTIC" project). AAF and MD acknowledge the ALISTORE European Research Institute for the funding support. AAF acknowledge Institut Universitaire de France for the support.

Keywords: lithium ion batteries • degradation mechanisms • analytical tool • dV/dQ • dQ/dV

- [1] C. Zhang, Y.-L. Wei, P.-F. Cao, M.-C. Lin, *Renewable Sustainable Energy Rev* **2018**, *82*, 3091–3106.
- [2] T. Kim, W. Song, D.-Y. Son, L. K. Ono, Y. Qi, *J. Mater. Chem. A* **2019**, *7*, 2942–2964.
- [3] N. Nitta, F. Wu, J. T. Lee, G. Yushin, *Mater. Today* **2015**, *18*, 252–264.
- [4] C. R. Birkl, M. R. Roberts, E. McTurk, P. G. Bruce, D. A. Howey, *J. Power Sources* **2017**, *341*, 373–386.
- [5] A. J. Smith, J. C. Burns, D. Xiong, J. R. Dahn, *J. Electrochem. Soc.* **2011**, *158*, A1136.
- [6] J. Vetter, P. Novák, M. R. Wagner, C. Veit, K.-C. Möller, J. O. Besenhard, M. Winter, M. Wohlfahrt-Mehrens, C. Vogler, A. Hammouche, *J. Power Sources* **2005**, *147*, 269–281.
- [7] J. Christensen, J. Newman, *J. Electrochem. Soc.* **2005**, *152*, A818.
- [8] A. Barai, K. Uddin, M. Dubarry, L. Somerville, A. McGordon, P. Jennings, I. Bloom, *Prog. Energy Combust. Sci.* **2019**, *72*, 1–31.
- [9] M. Dubarry, V. Svoboda, R. Hwu, B. Y. Liaw, *Electrochem. Solid-State Lett.* **2006**, *9*, A454.
- [10] M. Safari, C. Delacourt, *J. Electrochem. Soc.* **2011**, *158*, A1123.
- [11] C. S. Yoon, H.-H. Ryu, G.-T. Park, J.-H. Kim, K.-H. Kim, Y.-K. Sun, *J. Mater. Chem. A* **2018**, *6*, 4126–4132.
- [12] J. Li, J. Harlow, N. Stakheiko, N. Zhang, J. Paulsen, J. Dahn, *J. Electrochem. Soc.* **2018**, *165*, A2682.
- [13] D. Anseán, V. M. García, M. González, C. Blanco-Viejo, J. C. Viera, Y. F. Pulido, L. Sánchez, *IEEE Trans. Ind. Appl.* **2019**, *55*, 2992–3002.
- [14] M. Dubarry, C. Truchot, B. Y. Liaw, *J. Power Sources* **2012**, *219*, 204–216.
- [15] M. Dubarry, A. Devie, B. Y. Liaw, *J. Energy Power Sources* **2014**, *1*, 242–249.
- [16] A. Fly, R. Chen, *J. Energy Storage* **2020**, *29*, 101329.
- [17] I. Bloom, A. N. Jansen, D. P. Abraham, J. Knuth, S. A. Jones, V. S. Battaglia, G. L. Henriksen, *J. Power Sources* **2005**, *139*, 295–303.
- [18] I. Bloom, J. Christophersen, K. Gering, *J. Power Sources* **2005**, *139*, 304–313.
- [19] I. Bloom, J. P. Christophersen, D. P. Abraham, K. L. Gering, *J. Power Sources* **2006**, *157*, 537–542.
- [20] I. Bloom, L. K. Walker, J. K. Basco, D. P. Abraham, J. P. Christophersen, C. D. Ho, *J. Power Sources* **2010**, *195*, 877–882.
- [21] H. Dahn, A. Smith, J. Burns, D. Stevens, J. Dahn, *J. Electrochem. Soc.* **2012**, *159*, A1405–A1409.
- [22] A. J. Smith, H. M. Dahn, J. C. Burns, J. R. Dahn, *J. Electrochem. Soc.* **2012**, *159*, A705.
- [23] P. Keil, S. F. Schuster, J. Wilhelm, J. Travi, A. Hauser, R. C. Karl, A. Jossen, *J. Electrochem. Soc.* **2016**, *163*, A1872.
- [24] W. M. Dose, C. Xu, C. P. Grey, M. F. L. De Volder, *Cell Rep. Phys Sci.* **2020**, *1*, 100253.
- [25] D. Atkins, E. Ayerbe, A. Benayad, F. G. Capone, E. Capria, I. E. Castelli, I. Cekic-Laskovic, R. Ciria, L. Dudy, K. Edström, M. R. Johnson, H. Li, J. M. G. Lastra, M. L. De Souza, V. Meunier, M. Morcrette, H. Reichert, P. Simon, J.-P. Rueff, J. Sottmann, W. Wenzel, A. Grimaud, *Adv. Energy Mater.* **2022**, *12*, 2102687.
- [26] S. Wang, C. Pin, J. Yang, X. Wang, in *2019 IEEE 2nd International Conference on Electronics Technology (ICET)*, **2019**, pp. 543–546.
- [27] R. C. Limited, *PyQt5: Python Bindings for the Qt Cross Platform Application Toolkit (accessed 19 May 2022)*, n.d.
- [28] T. Zhang, S. Lund, T. Maruta, C. Y. J. Wong, *Proceedings of the North American Particle Accelerator Conference 2019, NAPAC2019*, 4 pages, 2.270 MB.
- [29] H. El-Bousiydy, T. Lombardo, E. N. Primo, M. Duquesnoy, M. Morcrette, P. Johansson, P. Simon, A. Grimaud, A. A. Franco, *Batteries Supercaps* **2021**, *4*, 758–766.
- [30] "Home - BIG-MAP," can be found under <https://www.big-map.eu/> (accessed 15 August 2022), n.d.
- [31] D. Atkins, E. Capria, K. Edström, T. Famprakis, A. Grimaud, Q. Jacquet, M. Johnson, A. Matic, P. Norby, H. Reichert, J.-P. Rueff, C. Villevieille, M. Wagemaker, S. Lyonnard, *Adv. Energy Mater.* **2022**, *12*, 2102694.
- [32] M. Fichtner, K. Edström, E. Ayerbe, M. Berecibar, A. Bhowmik, I. E. Castelli, S. Clark, R. Dominko, M. Erakca, A. A. Franco, A. Grimaud, B. Horstmann, A. Latz, H. Lorrmann, M. Meeus, R. Narayan, F. Pammer, J. Ruhland, H. Stein, T. Vegge, M. Weil, *Adv. Energy Mater.* **2022**, *12*, 2102904.
- [33] T. Vegge, J.-M. Tarascon, K. Edström, *Adv. Energy Mater.* **2021**, *11*, 2100362.
- [34] I. E. Castelli, D. J. Arismendi-Arrieta, A. Bhowmik, I. Cekic-Laskovic, S. Clark, R. Dominko, E. Flores, J. Flowers, K. Ulvskov Frederiksen, J. Friis, A. Grimaud, K. V. Hansen, L. J. Hardwick, K. Hermansson, L. Königer, H. Lauritzen, F. Le Cras, H. Li, S. Lyonnard, H. Lorrmann, N. Marzari, L. Niedzicki, G. Pizzi, F. Rahmanian, H. Stein, M. Uhrin, W. Wenzel, M. Winter, C. Wölke, T. Vegge, *Batteries Supercaps* **2021**, *4*, 1803–1812.
- [35] "EMMC ASBL | The European Materials Modelling Council," can be found under <https://emmc.eu/> (accessed 15 August 2022), n.d.

Entry for the Table of Contents



A software for electrochemical analysis of batteries: EVA allows further comprehension of the degradation mechanisms through a deeper view of the Potential vs. Capacity curves. The EVA functions, illustrated in its own simple interface, together with the guidelines presented in this concept paper turn the underexploited dQ/dV and dV/dQ curves study more intuitive and practical for researchers.